

INTERMODALITY NONRIGID BREAST-IMAGE REGISTRATION

Ioana Coman^{1,2,5}, Andrzej Krol^{2,3,5}, David Feiglin², Edward Lipson^{3,2,5}, James Mandel⁴, Karl Baum⁵, Mehmet Unlu⁵, Wei Li²

¹Department of Mathematics and Computer Science, Ithaca College

²Department of Radiology, SUNY Upstate Medical University

³Department of Physics, Syracuse University

⁴Department of Civil and Environmental Engineering, Syracuse University

⁵Department of Electrical Engineering and Computer Science, Syracuse University

ABSTRACT

We investigated nonrigid co-registration of PET and MR breast images to improve diagnostic specificity in difficult-to-interpret mammograms, and ultimately to avoid biopsy. A deformable breast model based on a finite-element method (FEM) was employed. The FEM “loads” were taken as the observed intermodal displacements of several fiducial skin markers placed on the breast and visible in PET and MRI. The analogy between orthogonal components of the displacement field and the temperature differences in a steady-state heat transfer (SSHT) in solids was adopted. The model allows estimation of the intermodal breast deformation for every location within the breast. To test our model, an elastic breast phantom with simulated internal “lesions” and external markers was imaged with PET and MRI. We estimated fiducial- and target-registration errors vs. number and location of the fiducials. We established that SSHT approach using external fiducial markers is accurate to within ~5 mm.

1. INTRODUCTION

Breast cancer is the most common malignant disease in women and the second leading cause of cancer death among American women today [1]. One of the major goals in breast cancer diagnosis is early detection of malignancy and its characterization. The main tool for detection and diagnosis of breast cancer is X-ray mammography. The normal follow-up diagnostic treatment following an equivocal or difficult-to-interpret screening mammography is surgical biopsy. Since majority of breast biopsies are negative (approximately 50% of biopsies are not needed [3]), it would be highly desirable to have an alternative, noninvasive approach as the second line of defense after mammography. For further differentiation other non-invasive imaging modalities, i.e. PET and MRI can be used. In this paper

we investigated a 3D FEM-based deformable breast model for intermodality (PET and MRI) nonrigid breast-image co-registration. This model estimates the displacement field for any location in the breast from observed displacements of external fiducial markers visible in both PET and MRI.

2. MATERIALS AND METHODS

For our experiments we used a custom-manufactured deformable breast phantom (CIRS Inc., Norfolk, VA; www.cirsinc.com), filled with medium-stiffness gel (vinyl-based hydrolymer with low concentration of nickel chloride) and surrounded by a skin made of thin urethane foil, see Fig. 1

The phantom was imaged using F-18 FDG positron emission tomography (PET) and high-resolution magnetic resonance imaging (MRI); for scan details see Table I.

Breast “lesions” visible in MRI were emulated by injection of oil (Johnson & Johnson) non-diffusing in the gel containing a mixture of organic azo dyes. F-18-FDG diluted in water-soluble gelatin with organic dyes was injected as close as possible to the “lesions” emulating lesions visible in PET. Six internal “lesions” could be uniquely identified in both PET and MRI (see Fig. 2).

TABLE I
IMAGING SPECIFICATIONS

	MRI	PET
Scanner	Philips 1.5 T, Intera	GE Advance
Scan Parameters	T1-weighted isotropic 3D FFE sequences with flip angle 20°	Transmission scan 3 min Emission scan 5 min
Spatial Resolution	0.7 mm	<7 mm
Acquisition/ Reconstruction matrix	512 × 512	128 × 128
Voxel size	0.7 × 0.7 × 1.12	4.25 × 4.25 × 4.25

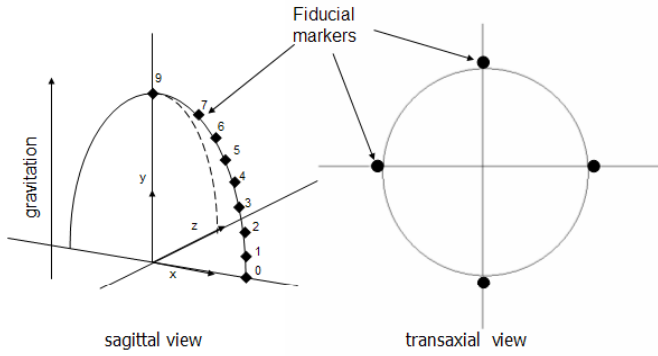


Fig. 1. Elastic breast phantom with external fiducial markers. Eight markers are placed on each four meridians and one additional marker is placed on the apex.

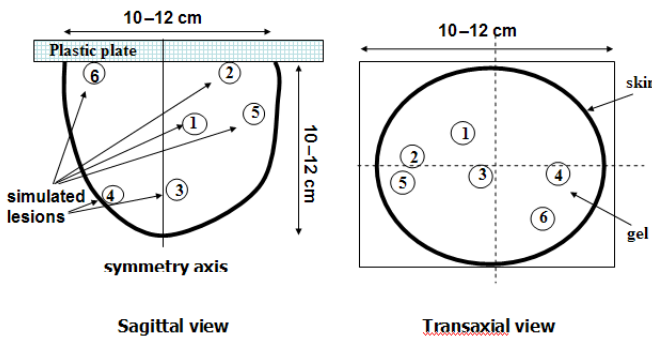


Fig. 2. Location of "lesions" inside elastic breast phantom.

3. MULTIMODALITY CO-REGISTRATION USING DEFORMABLE FEM-BASED MODEL

A deformable, finite-element method (FEM) based model of the elastic breast phantom was constructed [2], [4]. We assumed that stress conditions within the phantom were virtually the same for both modalities. This could be justified because the phantom was leveled and freely suspended in PET and MRI.

The analogy between orthogonal components of the displacement field and the temperature differences in a steady-state heat transfer (SSHT) in solids was adopted in our deformable FEM-based breast model. The model allows estimation of the intermodal breast deformation for every location within the breast from observed intermodal displacement of fiducial skin markers that are considered the FEM "loads". The displacement field components u_x , u_y , u_z are mathematically equivalent to temperature differences in the steady-state heat transfer problem and are all distributed linearly over the phantom domain. Figure 3 shows images of fiducial markers and "lesions" in the elastic breast phantom obtained using PET and MRI.

The geometry of the breast was obtained from MRI, and the meshing and FEM analysis were performed using the commercial software ANSYS¹. The following elements

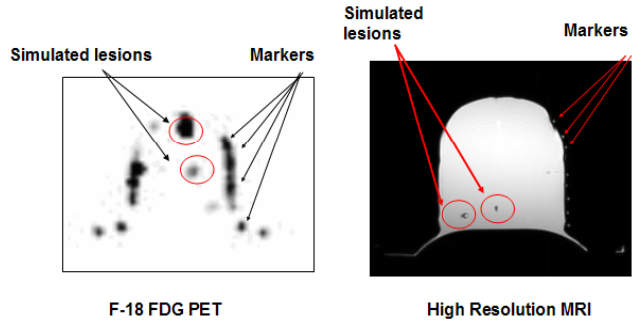


Fig. 3. Representative placement of "lesions" inside deformable breast phantom.

were chosen from the ANSYS library: *SOLID87* 3-D 10-Node Tetrahedral Thermal Solid; *SOLID70* 3-D Thermal Solid; and *SHELL57* 2-D Thermal Shell. A mesh containing a total of 15,636 nodes was created. *SOLID87* and *SOLID70* elements were used in the bulk of the object. The surface was meshed by a layer of *SHELL57* elements. The mesh used is shown in Fig. 4.

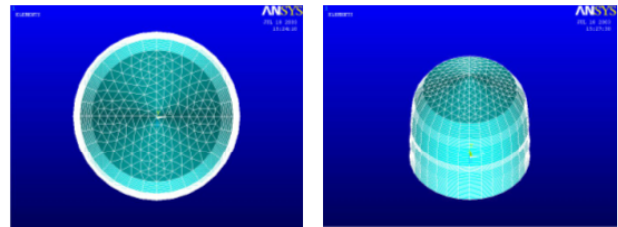


Fig. 4. FEM mesh generated by ANSYS software. *Left*: top view. The outer ring (white) shows shell elements. The inner ring shows brick elements. The central (and uppermost) area has tetrahedral elements. *Right*: oblique view. Brick elements are visible on the sides, and tetrahedral elements at and near the top

Thermal conductivity assigned to these surface elements was 1,000 times that used in the bulk of the phantom to assure that the surface layer reaches steady state 1,000 times faster than the interior. Intermodal displacements (between PET and MRI) for every location within the phantom were obtained. The execution time was 20 s per Cartesian component for the entire mesh using a 3 GHz, dual Xeon processor PC.

¹ANSYS, ver. 5.7, Inc., Canonsburg, PA)

4. RESULTS

We estimated two categories of errors: fiducial marker-registration error (FRE), and target-registration error (TRE); see Tables II and Fig. 5. FRE was estimated for the fiducial markers that were excluded from the registration process, while TRE was estimated for the internal “lesion”. We have established that intermodal elastic breast phantom co-registration performed using our SSHT deformable breast model with external fiducial markers is accurate to within ~5mm (voxel size in PET). TRE can be as large as two PET voxels, if proximal fiducial markers do not surround the “lesion”.

TABLE II
FIDUCIAL REGISTRATION ERRORS¹

No. of markers used in the FEM model	Mean Error (mm)	Standard Deviation (mm)	Min Error (mm)	Max Error (mm)
13	4.06	1.55	2.32	9.94
8	4.27	2.16	1.55	1.55
27 (all)	0.00007	0.00008	0.00002	0.00038

¹Fiducial registration errors (FRE, in mm) estimated using selected fiducial markers not used in the FEM model calculation for PET-MR co-registration. A total of 27 identifiable markers were available.

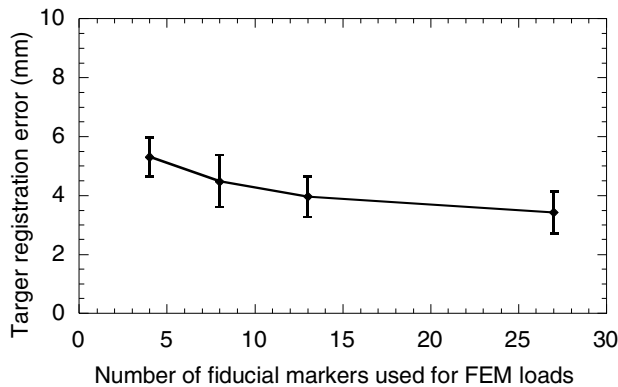


Fig. 5. Dependence of target registration error (TRE) on number of fiducial markers used in steady-state FEM model. Standard errors are shown based on six measurements for each point.

4. CONCLUSIONS

The SSHT deformable FEM-based breast model performs well for multimodality elastic breast phantom image co-registration. This co-registration procedure

requires external fiducial markers that have to surround the suspicious lesion and it requires very careful breast positioning to prevent change in the internal stress condition between different modalities. In the future work we plan to investigate how robust is this approach by intentionally introducing variation in the internal stress condition in the breast between different modalities and to study the influence of this factor on TRE.

5. REFERENCES

- [1] American Cancer Society (2002). *Cancer Facts and Figures* <http://www.cancer.org>
- [2] *Ansys Theory Reference* (1999) Eleventh Edition, SAS IP Inc.
- [3] C. J. Baines (1998). “Menstrual Cycle Variation in Mammographic Breast Density”. *Natl. J. Cancer Inst.*, 90, 875.
- [4] *The Finite Element Method: Basic Concepts and Applications* (Series in Computational and Physical Processes in Mechanics and Thermal Sciences), Hemisphere Publishing Corporation, 1992.
- [5] S. L. Sailer, J.G. Rosenman, M. Soltys, T. J. Cullip, J. Chen (1996). “Improving treatment planning accuracy through multimodality imaging”, *Int. J. Radiation Oncology*, 35, 117-124.